Mid-Wavelength Infra-Red Metalenses and Large-area All-Silicon Meta-optics

Vladimir Vladimirovich Yarmolik

A thesis submitted to fulfill the requirements of the degree of

Masters in Materials Science and Engineering

University of Washington

2024

Reading Committee:

Arka Majumdar

Navid Zobeiry

Program Authorized to Offer Degree:

Materials Science and Engineering

University of Washington

Abstract

Mid-Wavelength Infra-Red Metalenses and Large-area All-Silicon Meta-optics

Vladimir Vladimirovich Yarmolik

Chair of the Supervisory Committee:
Arka Majumdar
Department of Electrical and Computer Engineering

Mid-Wavelength Infra-Red (MWIR) meta-optics are an interesting research subject since these fabricated optics have uses in many fields and are at the core of some new technologies. Specifically, all silicon meta-optics that are fabricated on a thin 300 micron wafer cut thin and go through an electrochemical planarization from a 100mm diameter Silicon (100) crystal allow for compact and lightweight lenses. These properties, namely lightness, compactness, and high durability allow for uses in small unmanned aerial vehicles (UAVs), surveillance drones, infra-red cameras as well as wearable night vision goggles. Future applications can include smartphones, AR/VR, wearables, automotive, robotics, IoT platforms, as meta-lenses are optimal for presence detection, face identification, gesture recognition, eye-tracking, driver monitoring systems, and medical instrumentation. [1] In the core principle of the operation of meta-optic are the meta-atoms. The flat surface of the silicon wafer is patterned with structures called 'nanopillars' that are smaller than the wavelength of light that they are designed to manipulate. The pillars are usually made square so that their width and length is the same. The distance

between the pillars or how far apart they are is usually constant and is engineered so that they are effective at lensing the light in the specific optical regime (wavelength). In this work the meta-optics are designed to operate in MWIR regime, which is 3 to 5 um peak to peak wavelength thus the spacing between the pillars is 1.6 um between the 400nm pillars or 400nm between 1.6nm pillars necessary to pattern a hyperboloid meta-lens. The minimum feature size was 400 nm, which was pushing the resolution limit of our direct laser write system at Washington Nanofabrication Facility (WNF).

Outline

1. Introduction
2. Applications
3. Design and theory background
4. 400nm meta-atom fabrication challenges
5. Heidelberg direct laser write system exposure process development
6. Silicon etching process development
7. 2mm test apertures
8. 1cm and 2cm aperture fabrication
9. MWIR doublet (1st half) fabrication
10. Golay (piecewise) large area aperture fabrication
11. 8 cm aperture fabrication
12. Optical lab measurement setup
13. Optical Results: A Qualitative and Quantitative Study
14. Qualitative FLIR Images

1. Introduction

Meta-optics is a relatively new technology that found its uses in various industries that aims to transform the way lenses are used in the Infra-Red and Visible regimes. The technology is disruptive enough that it can be commended for bringing science fiction stories to reality in the form of everyday devices. The point when meta-lenses got traction and popularity was in the early 2000s, due to the conceptualization of a material with a negative refractive index that could be engineered to form a perfect lens. In the last five years it resulted in around three thousand publications a year [2]. This growth in popularity was further accelerated when Nature Photonics has commissioned a review from a group of industry and academics leaders in the meta-optics research such as Dragomir Neshev, Centre Director of the ARC Centre of Excellence for Transformative Meta-Optical Systems, and Professor Andrey Miroshnichenko from UNSW Canberra. The list of applications for meta-optics ranges from consumer optoelectronics applications to the Internet of Things, autonomous cars, wearable devices, augmented reality, and remote sensing. It was demonstrated that the technology is going into the consumer market when large scale investments started to come in from Apple, Google, and Samsung who began hiring engineers to research and engineer meta-optics for vision applications. Applications beyond vision can also include light sails, Light Fidelity (LiFi) and thermal management due to non-traditional characteristics of meta-optics. Namely, the characteristics are that meta-optics are surfaces that are patterned with 'nanopillars' that are nanoscale structures that are fraction of the size of the wavelength of light that they are designed to scatter and manipulate. Devices that integrate meta-optics as part of their design are already on the market, available from companies like NILT technologies, Metalenz, and Meta Materials Inc that offer flat meta-lenses for polarization imaging, microscopy and biosensing. Another novel application of these devices is

in quantum imaging senses and communications, where the meta-lenses can be uses to engineer and manipulate quantum states of light.

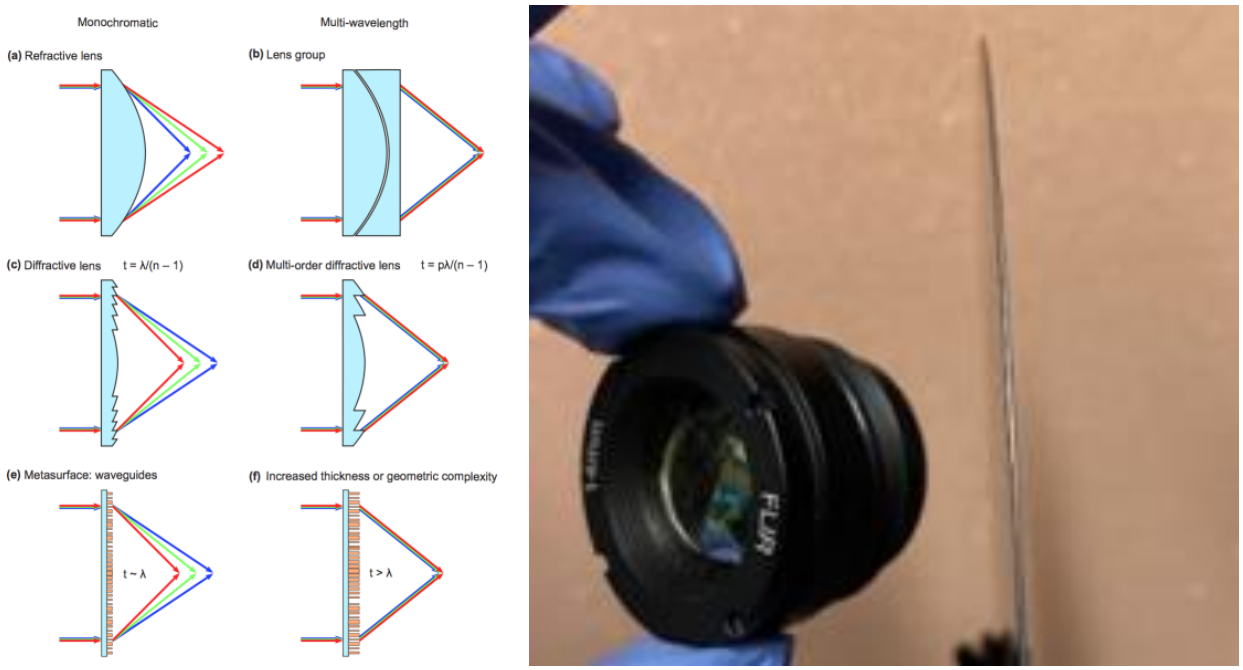

Figure 1: Left: meta optics as it is structurally compared to the other optics (Refractive lens top, diffractive Fresnel lens center, and metaoptic). Right: wafer with meta optic on it compared to the refractive compound lens

2. Applications

The specific applications which are usually mentioned in the projects of our lab include the space saving property of the meta optics and for MWIR meta optics specifically, the ability to image objects in the Infra Red regime. By using the known benefits of the meta optics, namely that the meta lens is much flatter: given that 100-500um is the thickness for the typical substrate onto which the meta lens is patterned, and the refractive compound lens can be several millimeters to multiple centimeters thick. An enormous benefit of meta optics is that not only the lenses come out thinner than refractive compound lenses, they are also cheaper.

Refractive compound lenses vs meta lenses

The two main pathways in which meta lenses are typically made cheaper are that they are simpler to manufacturing as they are flat wafers with meta lens pattern versus complex 3D lenses with aspherical lenses sometime included in refractive compound lens. Also, meta lenses do not require expensive materials like germanium, zinc selenide or calcium fluoride. To fully appreciate the cost savings that are associated with switching to meta lenses it is essential to demonstrate the degree of complexity of the field of refractive compound lenses. The scarcity of materials is emphasized by the fact that "there are numerous glass types available for the visible spectrum, but there are only a small number of materials that can be used in the MWIR and Long wave Infra Red (LWIR) spectral bands." [3] Materials used in these Infra Red optics are expensive, for example Germanium.

Germanium is a crystalline material and is a most common material out of which MWIR and LWIR refractive lenses are fabricated, however it is expensive. Germanium's intrinsic material property distinction is that it has a very high refractive index of 4.02. This fact allows to fabricate an optic with a large radius of curvature, meaning that a 3D optic can be 'flatter' compared to the one made with small radius of curvature. However, and additional complication with high refractive index for compound refractive optics is that a good anti-reflective coating is used to reduce reflection and improve transmission. Also, Germanium has a large change of refractive index with temperature at 396 parts per million per Kelvin (ppm/K). This large rate of change is a material drawback, as there may be a large focus shift with the change in temperature.

Magnesium Fluoride is a crystalline material that transmits light that is in the Ultra Violet wavelength range (UV) through visible and all the way to MWIR wavelength range. Also the

quality of the devices made from Magnesium Fluoride stands out as MgF2 has one of the highest transmittance values from all the materials used for making IR refractive compound lenses. Even though Magnesium Fluoride is significantly cheaper than Germanium, it is not always a better option as it has poor thermal properties. To make a lens out of Magnesium Fluoride one has to first grow it as a crystal or make it via "hot pressing."

Sapphire is another material that is prohibitively expensive. It is known for being extremely hard (with a hardness of 9) and thus cannot be diamond turned to form a lens. As a result it is very difficult and extremely expensive to manufacture. Instead of making IR lenses, Sapphire instead finds a niche application such as making up missile domes. Its optical properties are good however, boasting an almost as large of a range as Magnesium Fluoride (UV through MWIR) with a slightly lower transmittance than MgF2. Also, Sapphire has good thermal properties, and its refractive index does not change much with temperature at 13 parts per million per Kelvin. It also has very low thermal emissivity at high temperatures [3].

Finally, the last two alternatives listed here for making compound refractive IR lenses are Zinc Sulfide and Zinc Selenide. Zinc Selenide is much more expensive than Zinc Sulfide, but it offers a much higher transmission coefficient than Zinc Sulfide. The downside with Zinc Selenide is that it is structurally weaker, leading to lenses produced with this material ending up more fragile. Additionally, Zinc Selenide has a slightly higher refractive index, which necessitates a good anti-reflective (AR) coating for the lens to have a higher transmittance. Zinc Selenide works both in the IR and visible wavelength regimes, and Zinc Sulfide only works in Infra Red. Both materials have a reasonable value for the change in the refractive index with temperature at around 60 parts per million per Kelvin.

Fabrication of IR refractive compound lenses

In the world of glass fabrication methods the fabrication of Infra Red compound refractive lenses is generally similar to that of Visible range optics, with the exception that these exotic materials are sometimes more brittle, significantly harder than glass. Another important distinction that many of the materials for IR lenses are hygroscopic, or water absorbing which adds on another challenge in their fabrication If the material is too hard, it cannot be single point diamond turned, like Sapphire. This barrier significantly restricts design as it is then not possible to make aspheric lenses as part of the lens sandwich of the compound lens assembly. The good thing is that there are plenty of materials that can be diamond turned, such as germanium, zinc sulfide, and zinc selenide and calcium fluoride. [3] Since many of these materials however have an outstandingly high refractive index, a good anti reflection coatings are paramount. Without them naturally occurring Fresnel reflections take place and the device looses transmittance. Another layer of coating is necessary then to combat the hygroscopic nuance of these materials. Without waterproofing the lens with a coating any water contact will damage the lens beyond repair.

Endoscopes

Another application for the meta optics operating in the visible spectrum that takes full advantage of this space saving property is the tip of the endoscope. The procedure in which an endoscope is used to image or survey the normally inaccessible locations, like the inside of the patient's lungs is called endoscopy. A flexible wire portion of the endoscope with a small camera at the tip is inserted into the camera entry point of the patient (depending on procedure and usually requires an existing body orifice of the patient). The endoscope is thus guided inside the patient's body, carefully bypassing anything that is in the way of the endoscope camera and through the careful navigation of the twists and turns inside the patient's body the camera makes

its way to the destination. To simplify the motion of the endoscope through this complex three dimensional maze, instead envision a boat navigating a series of turns in a river. There are two boats, one is smaller and with a smaller turning radius, and the other boat is larger and can only make wide turns. While the small boat can just about navigate the twists and turns of the river, the river is too small for the other boat to pass through. Now imagine two endoscopes, one is equipped with a meta optic at the end, and another with a conventional refractive lens. The final device with a meta optic has a much more compact tip, allowing it to navigate inside the patient's body better and is able to access places in the body that are obscure and otherwise tough to navigate to. On the other hand, the endoscope with a refractive optic is too long and cannot turn as well, leaving some portions of the body wholly inaccessible and the endoscopy procedure cannot be completed. In the worst case scenario, if not done carefully, the long tip of the endoscope may damage the internal tissue of the patient, leading to the medical complications.

Other important applications involve the MWIR meta optics and their ability to see the unseen, in other words the capability of the camera equipped with a Infra Red meta lens in order to detect or image objects that are obscured or otherwise not visible to the conventional cameras that operate in the visible regime.

The technology behind the cameras that explains how the cameras are able to see objects that emit heat but are not visible to the human eye is called thermal vision. All objects that are above absolute zero (zero Kelvin) are emitting Blackbody Radiation.

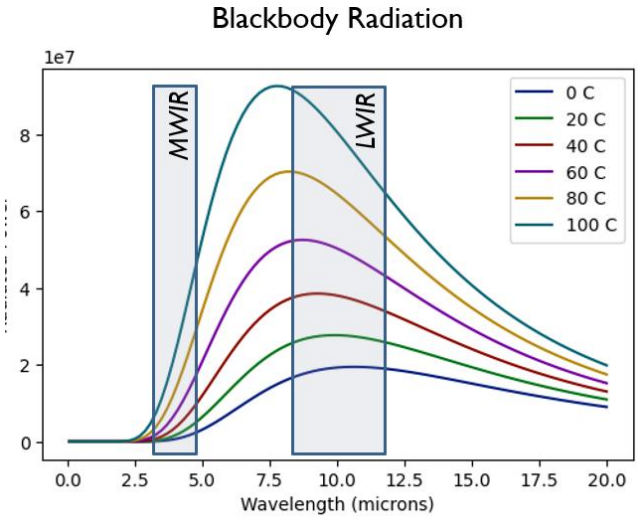

Figure 2: Wavelength spectrum of blackbody radiation with specific regimes portioned off

As shown in the Figure 2, blackbody radiation spectra were measured for comparatively hot objects (at zero degrees Celsius and above). One can note that the intensity of black body radiation for cooler objects drops off and forms a broader peak, but it is important to takeaway that black body radiation is ever-present and is a property of all hot objects. Specifically, the Mid-Wave Infra Red regime covers the wavelengths from 3 to 5um and Long-Wave Infra Red regime covers the wavelengths from 8-12um which leads to different meta optics design considerations. It is important to note that the ranges for Near Infra Red (NIR), MWIR, and LWIR are given by sharp drops in atmospheric transition due to the chemical components present in the atmosphere. [3] For example, a large portion of the MWIR band is isolated on one side by the drop in atmospheric transmittance due to the water absorption and on the other side by the CO2 absorption. This will be discussed further (in section 2), when talking about meta atom lattice and the widths and periodicity of the nanopillars that form the meta lens. From the Figure2 it also follows that if, for example, MWIR only operates from in 3-5um range of light and the visible spectrum is typically 400-700nm, meaning that a camera operating in the MWIR

regime does not need any optical light and thus can operate in complete darkness. This is a feature of "thermal vision" and the main distinction from "night vision". Night vision requires an optical source of light and uses image intensifier tube to collect more light that is reflected from objects illuminated by the built in green source of light. Another important advantage of thermal vision is that Infra Red cameras are designed to 'see; hear and thus detect radiation obscured by dispersed particles of smoke, dust, or fog, and are able to detect an object of shape that is obscured by a thin piece of material. They can also deduce the outline of the object behind that thin material. It especially helps if the thin piece of material is conductive and is placed close to the source emitting blackbody radiation. The thin piece of material will simply be charged up with heat from the hot source and an outline of the hot object will be visible.

Figure 3: Left: Outside image of the "W" monument taken with an infra-red camera. Right: same image but taken with a camera in a visible regime

Thermal Vision vs Night Vision

In order to further demonstrate the operating principles of MWIR meta optics, specifically their use at night, it is essential to compare and contrast Thermal Vision versus Night Vision. The

question is not to determine whether one is better than the other, because Thermal Vision and Night Vision have their own use cases and advantages.

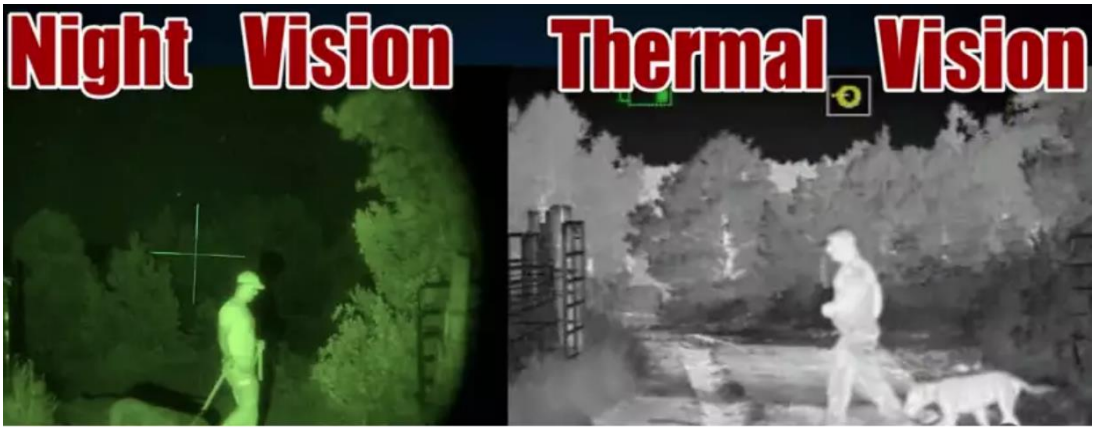

Figure 4: Visual comparison between Night Vision and Thermal Vision. Heaton, Wyatt. "Night Vision vs. Thermal Optics: What You Need to Know."

First, one must consider the true capabilities of each in order to know in which situation it is best to utilize either of the devices. This is not necessarily a discussion on the performance of the specific model of the device, as different models will be priced differently based on the cost of manufacturing of the device and how custom built the device is. In its core principle, thermal vision requires a Forward Looking Infra Red (FLIR) camera whose sensor input is then converted to an optical (visible range) output in the grayscale format. Hot objects appear in bright white, while cold objects appear in perfect black. One important thing to mention here, is that there is no fundamental color associated with how hot the object is, as this sensitivity to heat can be calibrated in the camera setting. Collected Infra Red rays are converted into a thermal image using a unique electronic system, which transforms the electrical impulses created based on the IR radiation received by the device and displays the finished result on the optics display. [4] Additionally, there is another control knob if the FLIR camera has a range of wavelengths

that it can work with. One can set up the camera to only detect a specific wavelength based on the use case application. There is also a big drawback because of the fact that Thermal Vision utilizes a camera necessary for its operation. The camera sensor has a limit on how big it can be and how many pixels it has, in other words, the resolution of the camera sensor. Assuming the same pixel size, which is usually measured in microns, the bigger the sensor and better is the resolution. For reference here the FLIR camera sensor of the camera used to characterize the devices fabricated for this work has the resolution of 640 by 512 pixels and exact model is FLIR A6751 MWIR Cooled InSb, with the pixel size of 15 microns. If, for example, one were to use a more compact sensor with a smaller diagonal dimension but the pixel size would remain to be 15 microns, the quality of the image for the user would decrease. What is even worse, is that since that the image is digital in nature, and the resolution decreases with the increase in magnification, user experience with Thermal Vision may be unsatisfactory at high magnification. It is known that with the FLIR camera there are additional detrimental visual artifacts when zooming in on the object in front of the camera. The image appears grainy, as there is additional pixel noise that gets introduced at higher magnification values. This is analogous to the digitized image coming from a cell phone camera. At the zoom level of 2.0x there is only 0.5x of the resolution or the pixel count of the image which introduces the defects such as blurriness or jagged edges. Despite the fundamental issue Thermal Imaging being a digital representation of the scene in front of the observer, this technology can be a vast improvement over the unaided eyesight when viewing objects at night. It is hugely beneficial for surveying, tracking, hunting, and security observations. Since Thermal Vision is valuable in these applications, there is a push for fabricating better devices and there is a great demand for thermal imaging development. Currently there is a problem with weight and the fact that Thermal Vision devices are bigger than

Night Vision device counterparts. The design of the thermal imaging models contains lenses of a larger diameter than NV optics, [4] which forces the manufacturers to increase the overall dimensions of the product. This thesis work aims to help with this, as the meta optics can be proven as a solution to bulky compound refractive lenses used in the current design of the Thermal Vision goggles.

Night Vision is different in its core principle of operation as it not a digital system, but it is an optical system. This means that before the light passes through image intensifier tube, the image is accurate and the resolution is only limited by how good the user eyesight is. A good comparison is an optical magnification one can get from the binoculars. The image remains crystal clear, with no defects, albeit just magnified. Then, image intensifier tube is used to capture light an to amplify it. Various manipulations with light happen to produce a brighter and a somewhat more transparent image. Night Vision Device (NVD) have an intensifier tube built in, as it serves a critical role for the operation of this device. It converts the light the device collects into an image the human eye can see. [4] The main drawback of the Night Vision is that it is only useful in the dark. The image appears simply too bright, if the device is being used if there is sun present, or even any other artificial lights. Furthermore, it is often the case that there is not enough light for the NVDs to operate. Any natural light such as stars and the moon will actually aid the performance of the Night Vision. However, even with natural light and if natural light is aided bey some artificial lighting, it is still very difficult to see in the shade of an object. In complete darkness, and without any additional illumination, NVD becomes practically a useless optic. To combat this, NVDs are equipped with an Infra Red illuminator. This is an additional built in element that is required to compensate for the lack of natural light or to be able to see in the shadow of the object. Light from the IR illuminator is then compounded in the

optics of the NVD in order to produce a complete and brighter image. From Figure 4 it is also evident that the shadow is visible from the light source of light from the IR illuminator as part of the night vision goggles.

Thermal Vision for security and surveillance

Another important application for IR cameras is aerial video surveillance. If it is dark outside or if aerial surveillance is otherwise impossible due to a heavy fog or haze, the go-to solution is to use an Infra Red camera. Since thermal imaging is becoming essential nowadays, there is a growing interest for smaller and lighter cameras. Since mete lenses are many times thinner and lighter than refractive compound lenses they make for a great fit onto a light surveillance drone. A thermal vision camera mounted on a drone can be potentially a life saving combination and has a number of use case scenarios which are going to be explored here.

Firefighters, for example, have a history of using thermal cameras basically since those cameras became available. Since traditional cameras that operate in the visible wavelength regime become practically useless if there is something smoldering in the darkness, especially if there is a lot of smoke present too. In absolute darkness and obscured in smoke the firefighters are able to locate and extinguish a hot spot, whether it is out in the open or in building floor, wall, or ceiling. “The ability to see through the smoke with an infrared camera contributes to secure sites and to help saving lives” [5] Since time is of the essence and firefighting process is usually an intervention in a home or business scenario, the speed and efficiency become first priority. Firefighters rely on the powerful features of IR cameras to search for victims, detect fires even if they are light or residual, neutralizing a hot spot even after the fire. Most importantly, IR cameras can be used when working to find a person in the rubble, or in case of a traffic accident at night to find a body that has been ejected from the road.

Coast guards and rescue crews at sea have been also increasingly using the Infra Red cameras to save lives. In the case if a person has fallen out of the sea vessel they must be recovered quickly at all cost. The danger with open water mayday scenarios like that is that as time passes a person ends up further from the vessel and the chances of their rescue decrease dramatically. Additionally, the accident at sea when a person has fallen out from the vessel results in the victim becoming hypothermic as the cold sea weather and exposure to elements render the body unable to keep waiting for the rescue. If thermal vision is applied however, the person washed away at see becomes a bright dot in the darker, colder water which leads to a quick recovery of the person in distress.

For applications that are not quite about saving lives, but nonetheless are still important, the police customs officials use thermal imaging for night operation. There is a number of videos on the internet where suspects are intercepted by police on the boarder thanks to the surveillance of IR security cameras. The functionality of the cameras allows them to operate in complete darkness and the thermal gradient on the camera output allows for easy tracking of suspects. Due to the Thermal Vision suspects cannot hide in bushes or in the shade because the cameras can "see" heat and police officers are able to find them immediately. "Moreover, thermal imaging helps securing places of intervention for police and security forces by increasing the knowledge of the field and by locating threats present in the operational area" [5]

In case where human lives are not necessarily in stake but instead the question is about profit, for industrial applications use IR cameras to mitigate severe dangers, reduce losses due to theft and have an otherwise need for security. The users of thermal vision surveillance are nuclear power plants , petrochemical refineries and installations, warehouses storing or managing expensive assets. Lightweight IR cameras that require lightweight lenses already have their demand.

Thermal cameras for autonomous driving

Finally, this work features an application of thermal vision cameras for the purpose of driverless navigation or autonomous cars. Thermal cameras are fundamentally different from LiDAR (Light Detection and Ranging), where the laser pulse is sent in the environment and the precise timing of collecting the returning light allows to discern the shapes obscured by foliage. At the core of the Infra Red camera there is a sensor, sometimes called micro-bolometer. A sensor is made from silicon and applies CMOS technologies to measure the scene temperature and represents a temperature coming from a point on the scene by a pixel on the camera screen. It happens to be that the pixels are "sensitive to radiant thermal energy, which changes the electrical resistance and enables measurement of a scene temperature" [6]

Before micro-bolometers there were bolometers. Invented in the 1970s by the company Honeywell for the US Department of Defense under a classified contract this development eventually led to Long-Wave Infra Red (LWIR) cameras for ISR (Intelligence, Surveillance, Reconnaissance). The Long Wave regime is more forgiving as it allows for larger parts involved in the microfabrication. As bolometers are basically arrays of pixels that are used to provide thermal contrast images of a scene. Later the bolometers and other portions of the technology were declassified in the 1990s. As soon as they were declassified there were commercial entities that wanted to use the technology. And now, the thermal imaging application ranges from defense and boarder surveillance to remote temperature monitoring (hugely popular during COVID) and to nighttime driving.

Micro-bolometers work in a different Infra Red regime than MWIR optics, as they are sensitive to light in the wavelength regime from 7.5 to 14um. However, both LWIR and MWIR have the capability of capturing the blackbody radiation (see Figure 2) and therefore MWIR optics are

still applicable to autonomous driving sensing systems. What makes micro-bolometers a great fit for this advanced vehicular application is that they can easily pick up body heat of animals and humans at long ranges from the driver. Detecting these heat signals and identifying them as different from all other objects natural or artificial that typically appear in the scene is essential for safety of autonomous vehicles. Additionally, measuring these temperature differences with micro-bolometers allows to cover the "corner cases" where all other sensors are not supplying sufficient information for the autonomous car navigation system.

Using thermal cameras on vehicles is not necessarily a new concept. Back in the 2000s several car manufacturers such as BMW, GM, Honda and others were installing passive thermal cameras to assist the driver and provide additional safety under nighttime conditions. These were primarily to avoid animal collisions or injuring pedestrians in situations of heavy mist or fog or insufficient lighting at night. However, the autonomous car sensing system has improved since then with an addition of LiDAR in order to advance through the levels towards fully autonomous driving (L4). As introduced by DARPA Grand challenge, level 3 is considered conditional autonomy where the driver is present to take control of the vehicle manually with a 10 second warning and L4 is full autonomy under Operational Design Domain.

The realization of L4 autonomous driving is a difficult process and requires further development of the "ideal stack" of sensing equipment and then making said sensing equipment cheaper in order for mass adaption of the technology. There is now a competition to develop a cheaper FLIR camera, starting with its center. Even though the supply chain is already well developed in US, Europe, Korea, Japan, and China, the sensor market is dominated by Teledyne-FLIR. FLIR company provided some of the initial sensor capabilities used for human driver assistance used by BMW.

Figure 5: A pedestrian is completely obscured by smoke during daytime. A FLIR camera is still able to detect them. Rangwala, Sabbir. "Thermal Cameras Gain Acceptance for ADAS and Autonomous Cars." Forbes

"Today, Teledyne-FLIR is a dominant provider of LWIR thermal cameras for a wide range of applications from firefighting and security to drones and automobiles" [6] They produce miniature thermal cameras that are now in the 4th generation in the VGA (Video Graphics Array)/ The resolution is 640x512 pixels and the pixel pitch (the distance between the pixels) is 12um.

In order to bring a cheap cameras to millions of cars on the road one must also consider the optics used in thermal cameras. Even though Germanium is ideal for LWIR cameras, and is the military standard, it is expensive. Over 90% of Germanium reserves are located in China and Russia and given the geopolitical environment, it can become a major supply chain concern. However, since it is projected that thermal camera use in cars (even human driven) will be drastically increases, there is a push to create a much more cost-sensitive solution and the cost per camera should fall below $100. Specifically, for the Infra Red optics, one pathway is volume

scalability: unlike Germanium that needs to be machined, glass lenses can be molded in large batches leading to higher production volumes and lower capital and labor costs. As explored previously in this work, germanium has a high refractive index change with temperature rate, and has transmittance losses that vary substantially over operating temperature range for automotive from -40C to +85C. As for the molded glass optics, Chalcogenide glass can be employed as a less dense solution to Germanium and is already pursued by the company Umicore in terms of material formulation and lens fabrication.

However, both Germanium and Chalcogenide glass are both bulky solution to the optics problem in lens fabrication for autonomous car thermal cameras. The fabrication of flat, thin and light meta optics described in this thesis is a space saving and less weighty contender to use in all the cases where there is a need for compact solution for Thermal Vision applications.

3. Design and theory background. MWIR meta lens process development

Initially, when the fabrication process was not yet established there was an issue in achieving the 400nm meta-atom size. Previously, this MWIR process was demonstrated by Zheyi Han using the stepper photolithography tool for the write step. However, due to the limitations, namely, WNF selling the stepper tool as used equipment, there was a need to find another tool for the write step. Heidelberg DWL 66+, a direct laser write photolithography tool was the next solution, since with the High-Res head installed the theoretical limit was 300-500nm minimum feature size, which suited the needs of this project.

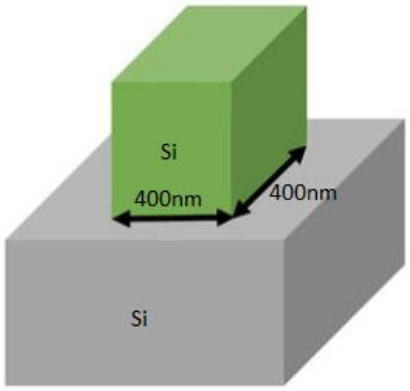

Figure 6: Primitive unit cell of nanopillar lattice with dimensions of the meta-atom

4. 400nm meta-atom fabrication challenges

Heidelberg DWL 66+ uses GDS (Graphic Design System) files, specifically in GDSII file format, as will be discussed later. As mentioned in the introduction and later in the application section of this work, the design has a 2D map of nanopillar lattice based on which silicon is etched and a layer structure is then later fabricated giving nanopillars their height. In order to apply the principles of Materials Science and Engineering, Figure 6 represents a primitive unit cell of the nanopillar lattice. Primitive in this context means that if this block of silicon, which is the smallest possible repeatable unit of lattice, if translated correctly forms fills a lattice space without any overlapping or voids. Repeating this primitive unit cell in the x and y axis as indicated by the black arrows forms a complete nanopillar lattice. A 2D lattice with a periodicity that is equal in x and y, or the one with a square base is has been defined in Materials Science and has a special name. It is a Tetragonal Bravais Lattice with a D4 point group. A Bravais lattice, named after Auguste Bravais is an infinite array of discrete points formed by discrete translation operations described in N-dimensional space.

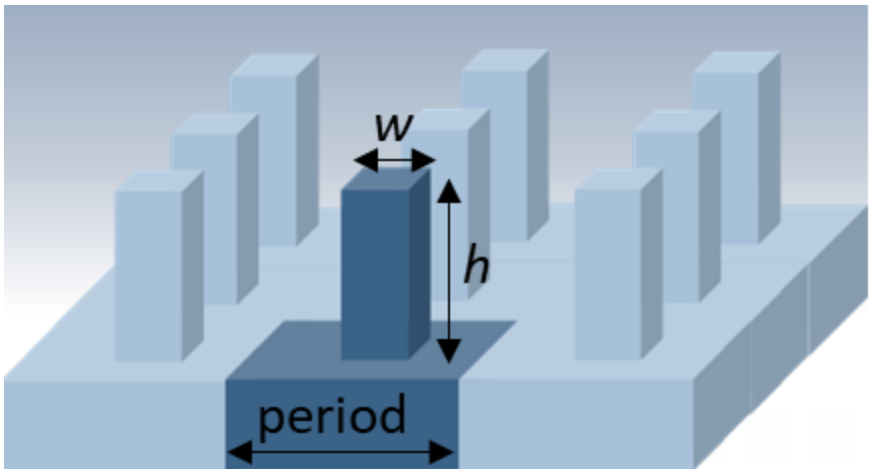

Figure 7: Repeated nanopillars forming a complete lattice

However, there is one caveat about forming the lattice for the purposes of forming a meta lens. First of all the lattice is not infinite, it is always bound by the dimensions of the silicon wafer, upon which the GDS design containing the nanopillar lattice is patterned. It is often desired to fabricate a set of smaller lenses that all fit on the same wafer and have those meta lenses be written in one photolithography step in parallel. The smallest meta lens fabricated for this work was 2mm circular lens. Additionally, in order for the circular meta lens to be efficient in modifying the incoming Infra Red light, the nanopillar aggregate must me fashioned in something known as a hyperboloid. Hyperboloid is the name of the phase profile shape which is in theory has the best performance at one wavelength of light and does not result in any aberration for monochromatic light. In this thesis, all the fabricated meta lenses are optimized to work with one wavelength, so the nanopillar patterns are all fashioned into hyperboloids. The only exceptions to this was a doublet and a broadband version of the Golay lens, which was designed to work with a broadband (multiple wavelengths) source of light. In other words, when forming a hyperboloid out of nanopillar lattice, it was chosen to keep the same height for all pillars, h (Figure 7), and to keep the period of the pillars the same and only change the width of

the pillar w, which is the same in the x and y axis. As a result the smallest pillars that needed to be fabricated were 400nm and the period of 2um (2000nm) leaved 1600nm as the distance between the pillars. The width of the pillars varies however throughout the circular meta lens and the width w can be as large as 1600nm, leaving only 400nm gap between the pillars. Both 400nm pillars and forming a 400nm gap between the pillars was a challenging thing to achieve, as will be discussed later. However, as also is discussed below, selecting the smallest possible nanopillar width that the particular write head allows is beneficial for final device image quality. Another benefit is that it is better to have small pillar and large gap of air between them rather than have a large pillar and a small air gap between them because the large pillar and small gap scenario creates unwanted resonances. These resonances make the phase graph (red line) slope steeper and the transmission (blue line) values lower.

Another crucial reason why different feature sizes were included in the design were to create what is known as a phase profile. A range of possible phase shifts (indicated on the y axis of figure 8) needs to cover the range between 0 and 2π, in order for the meta lens to be effective at modifying and 'steering' the incoming light. On the x axis there is a there is a range of feature sizes, between 1.6 and 2.4 um. It is important to note that the meta lens is this case is designed to operate with a single wavelength of IR light, specifically 4.5 um. All of the feature sizes are smaller than the operating wavelength. Ideally, the period, which incorporates the feature as discussed in the primitive unit cell example, should be half the wavelength (at around 2 microns) or smaller in order to avoid higher-order diffraction. However, since all-Si scatterers are forgiving in the fabrication step and there is actually sufficient design freedom to have the period (or periodicity) of the unit cells to be much larger that half the wavelength of light. Whenever the fabricated lens was larger that 2cm in diameter, it was a necessity to switch to a larger, but

lower resolution write head. At the extreme end, if the meta lens occupies entire wafer, with a little bit of space left for wafer handling with cleanroom tweezers, the write times increase by a factor of ten based on the write head size. In the case of 20mm head, such write will only take 35 minutes but will be entirely unsuitable for MWIR meta lens fabrication because of its low resolution. For 4mm head the write time is about 6 hours for the whole wafer, or about 360 minutes. It was tested by another user during an all weekend run that the longest possible write before the software crash with a high resolution head (2mm) was 61 hours. A write head can be thought of as an operating tip of the direct laser write system that is Heidelberg DWL 66+. The larger the head size, for example 4mm (low res) versus 2mm (high res) the lower the write resolution, but the faster the write time. Because there were many users who reserve the tool in Washington Nanofabrication Facility (WNF) there is a general need to keep the reservation times and thus the write times short. All of the writes presented in this work were done during overnight reservation slots or during shorter, daytime reservation slots. This policy results in another design constraint and thus dictates the write head size used for the meta lens writes.

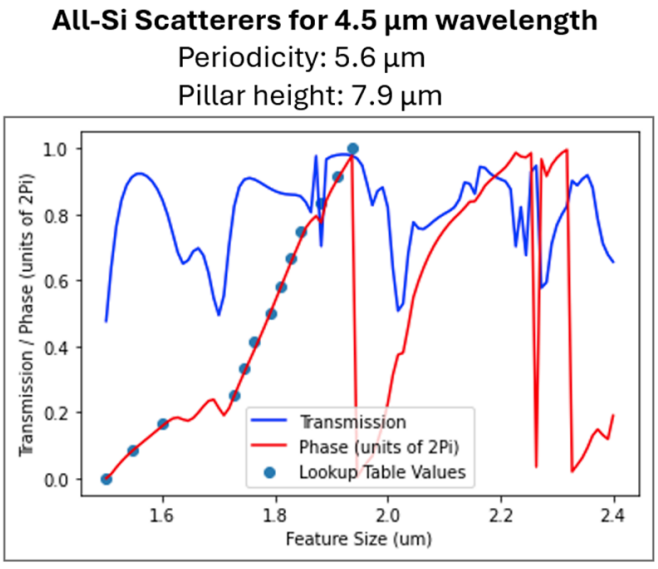

Figure 8: Phase profile for any MWIR meta lens that was fabricated with 4mm write head

For the reader to gain an understanding into how this graph was generated and to understand how the incoming light perceives the meta lens and what makes it effective at modifying, steering, and lensing light it is important to discuss the 'net effect' of the fabricated features on this all-silicon scatterer presented in Figure 8. A well designed meta lens allows the incoming light to 'see' the meta lens not as a series of nanopillars and air (gaps between the pillars) but rather as a net effect of the unit cell. If the unit cell is small enough relative to the wavelength, the light experiences the net effect, or an effective combination of the air and pillar. However, if the meta lens is improperly designed and the unit cell is much larger than the wavelength of IR light, then the light might scatter and diffract off of the interface between the pillar and the air rather going past it.

The turquoise dots on the graph that lie closely to the red line indicate the actual lookup table values that were used for the feature size for the design that was later used in the GDS file for the write using Heidelberg DWL 66+. This is a faster way to do the design, and since the simulation of the feature size varying across the meta lens is a lengthy process, a look up table that gives a feature size to cover the phase shift profile from 0 to 2π is a nice convenience that also speeds up the process when coming up with a new meta lens design. One should note that the continuous graph of phase versus the feature size (red line) also gives a complete phase distribution for features that are larger than 2 microns. Even though it is possible to design a meta lens using the look up table values for the this larger set of feature sizes, the resulting meta lens will be less desirable for the following reasons. First, the smaller the nanopillar size (if it is possible to still reliably fabricate them) the better, since during the testing of the meta lens in an actual lab setting, the lenses with smaller feature size will provide a better image quality at the same aperture diameter. The rule of thumb that can be later discerned from the images of the actual

meta lenses fabricated for this work, a 5mm lens with a smallest possible feature size fabricated using the high resolution head provides about the same image quality ans a 20mm lens with smallest possible feature size fabricated using 4mm (low res) write head. The second reason notable on the Figure 8 graph is that the red line only gives features from about 1.9-2.2um for the phase shift of 0 to 2π and may result in another challenge of actually forming a hyperboloid lens for testing. This gives rise to a limited feature size constraint for the design which can be eliminated by just selecting a region with a flatter red line slope which also happens to have smaller feature size as denoted by the overlaid turquoise dots on Figure 8 graph.

Figure 8 also lists the pillar (nanopillar) height to be 7.9um. This value was determined from carefully simulating the all-silicon scatterer based on the feature sizes and the periodicity. It is possible that other etch heights are possible given other set of combinations of nanopillar size and periodicity. The benchmark for the simulation was for the fabricated device to cover the phase shift from 0 to 2π. It was found that when the periodicity was made larger, to be compatible with writing using the 4mm head, the nanopillar height was needed to be increased to a target 7.9umm in order to cover 0 to 2π phase shift. In this case the height is chosen to be 7.9um and it dictates the etch depth into the silicon substrate during the Deep Reactive Ion Etching (DRIE) step of the meta lens fabrication. Achieving this etch depth while keeping the sidewall profile vertical was a challenge that was solved for this fabrication task and will be discussed in the further sections of this work.

5. Heidelberg direct laser write system exposure process development

During the MWIR fabrication process, in testing of the High-Res head a severe striping issue was discovered (Figure 9). After bringing the issue to the tool supervisor, the solution was found. When preparing the job for the write, in the exposure parameter window, there is an

option to select the CD bias. Initial setting is 0nm in the both x and y direction. After consulting with the tool supervisor a decision was made to set the CD bias to -100nm in x and -100nm in y direction.

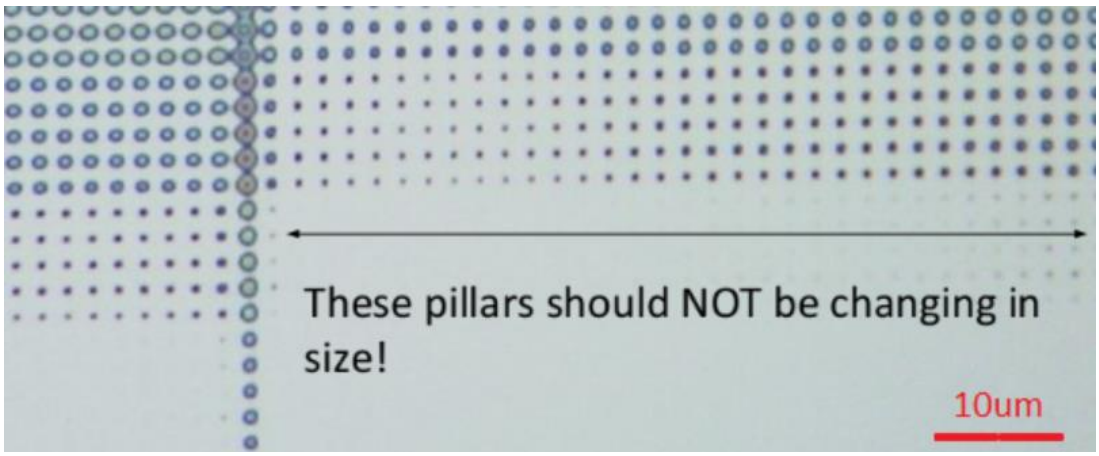

Figure 9: Striping issue

6. Silicon etching process development

The second issue that came up was the collapse of the meta-atom pillars after the etch step. The tool that was selected for the etch step was SPTS with capability of Deep Reactive Ion Etching (DRIE) also know as Bosch process. Initially, a polymer lean recipe was used, as it was the standard recipe to use in the tool, ensuring the process chamber walls being clean of the C4F8 polymer that is used in the deposition step of the Bosch process. This polymer lean recipe leads to negative sidewall profile as in the progression of the etch less and less deposited polymer makes it in the bottom of the trench between the pillars. (Figure 10).

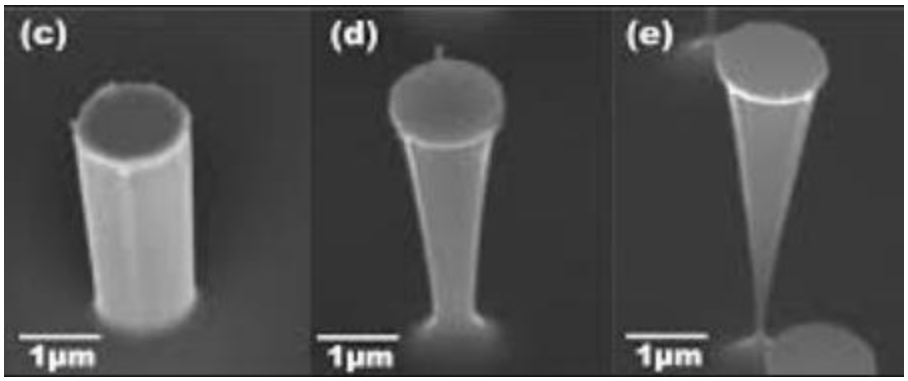

Figure 10: Negative overhang in DRIE A. Ayari-Kanoun et al. "Silicon nanostructures with very large negatively tapered profile" Journal of Vacuum Science & Technology B

However, as our feature size is so small (400nm), even a relatively shallow etch of 6 loops (3um) was sufficient to undercut the nanopillars enough that they collapsed (Figure 11). To combat this, we discussed our issue with the tool supervisor, and they informed us that it possible to alter the recipe to make the sidewall profile more vertical. The solution was to increase the deposition of C4F8 from 1 to 2 seconds, keeping the first SF6 etch step the same 1 sec, and reducing the second etch step from 2 seconds to 1.5 seconds. This effectively allows for more deposited polymer to prevent the sidewall etching as well as reducing the time for isotropic etching to undercut the sidewalls.

Figure 11: Pillars collapsing issue

SEM of first successful device is presented below: on figure 12A a zoomed out view of the device with no pillars collapsed and figure 12B offers a zoomed in and tilted view of one of the nanopillars capturing the individual scallops (10 in total).

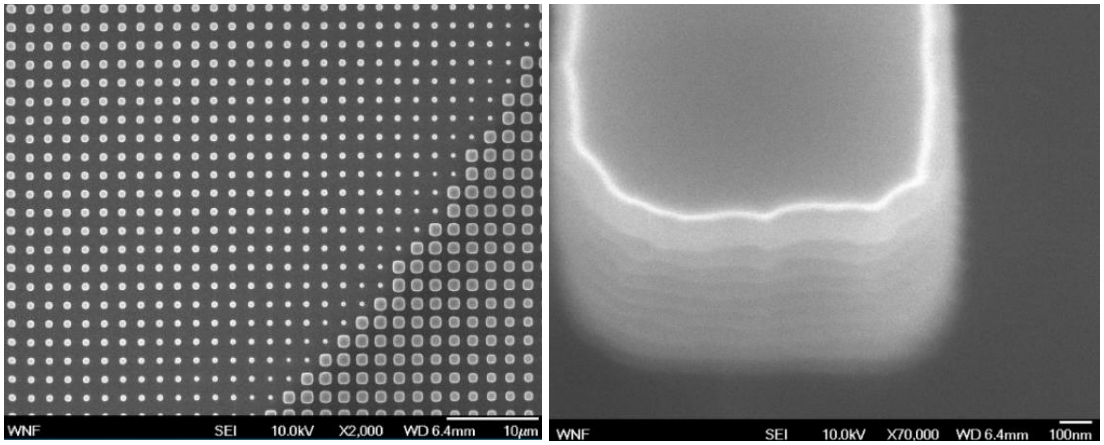

Figure 12A (left) and **Figure 12B** (right)

Here is an important reason why the Heidelberg write parameters need to be checked every month. During the time it took to make various designs presented in this work the Heidelberg intensity parameters shifted by as much as 20 percent. The image below is taken after the development of the test lens written with high res head (2mm). The intensity of this lens in the array of lenses that make up the focus/intensity matrix was set to 50 percent. Upon development that about 50 percent of the pillars have collapsed or no longer exist due to the photoresist nanopillars being to thin. Intensity was further optimized to the point the photoresist was forming a good photomask to proceed with the next step, which is etching. Etching process optimization was already discussed in this section.

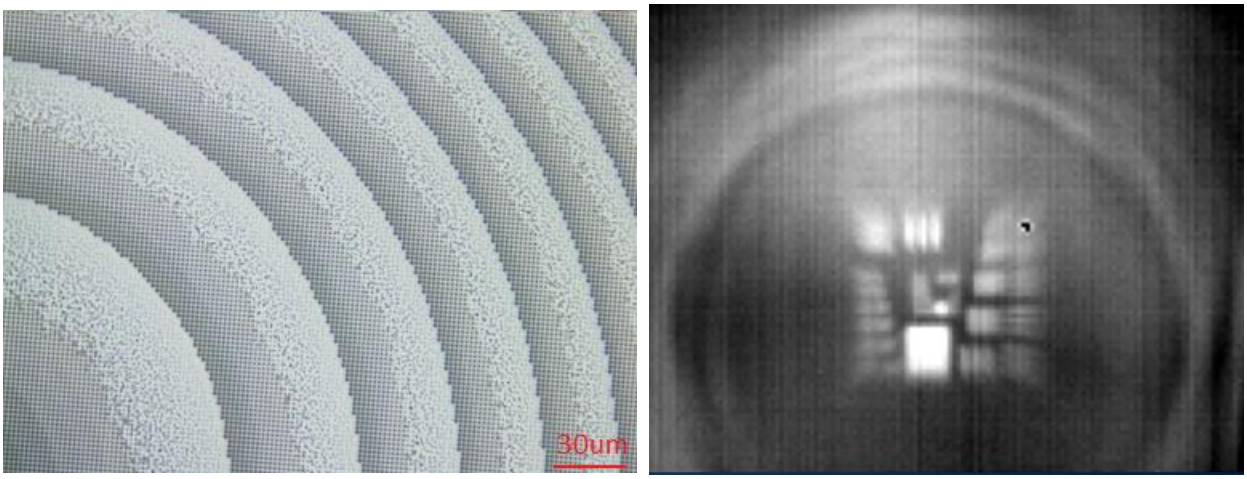

Figure 13: A more extreme exaple of pillar collapse. Optical microscope image (left). Image taken with FLIR camera (right)

7. 2mm aperture process development and fabrication

The fabrication starts from the 2D GDS pattern which represents a file format that in itself is a layout of planar geometric shapes and other rectangles that makeup text labels and actual meta-atoms in a hierarchical format. The GDS is then written using a direct laser write system Heidelberg DWL 66+ which exposed a layer of AZ1505 positive photoresist sensitive to ultraviolet laser light. The wafer is then developed in AZ726 photoresist developer for 1 minute. In this step the pattern written with the laser is revealed and the photoresist becomes a photomask for the etching step. The exposed areas of Silicon are then etched in Deep Reactive Ion Etch (DRIE) system to a desired depth of either 3um in case of the MWIR meta lens or 5um in case of MWIR doublet. Following the etch step, the wafer is inspected in a Scanning Electron Microscope (SEM) to verify the quality of the fabrication process in which any meta-atom pillars that collapsed from DRIE can be seen. Finally, the SEM inspected wafer is taken to the optics lab and to record the devices' quantitative and qualitative performance. The quantitative

performance is measured by Point Spread Function (PSF), using a point source which is an infra-red laser, the device is then benchmarked on how well it can focus laser light into a point. Intensity of light at a point is then measured to give a quantifiable result. The qualitative performance is measured using a Forward Looking Infra-Red (FLIR) camera, using a hotplate and USAF target as a source of light. The image recorded by FLIR camera is then judged by the operator on how sharp the image is, compared to standard diffractive optic.

8. 1cm and 2cm aperture fabrication

The fabrication process of 1cm and 2cm was basically identical, for the one difference in the starting GDS file. For the case of 1 cm aperture, four different designs were combined in one GDS, which were consequently fitted onto the same wafer. Namely the designs included 5mm Hyperboloid lens. There was an interest in testing a 5cm lens in an optical lab since its diameter lies in the range between 2mm and 10mm. This is why the 5cm lens was also included in the 1cm GDS.

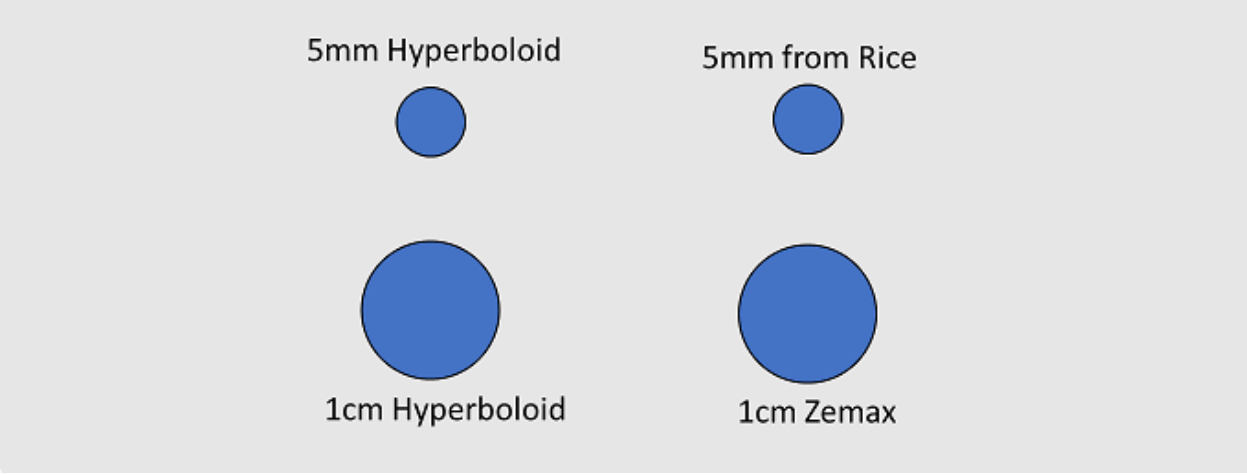

Figure 14: Cartoon of 1cm lens GDS

On the 2cm lens GDS there were also 4 individual lenses. Two 5mm lenses were included for the optical lab test purposes. 2mm lens was a nice convenience since it was placed in the center of

the wafer, which made it easier for the focusing using the JEOL SEM to find the rough focus on the target meta-atoms. One can also notice from the raw GDS file on [Figure 14] that there are labels included in the design, namely "2cm F1" next to the 2cm lens as well as "5mm F1" and "5mm F4" which proved later to be another convenience later when using optical equipment in the lab in order to find the surface of the wafer as imaged by the FLIR camera. The salmon colored circles are meta lenses with individual meta-atoms too small to be seen at this scale.

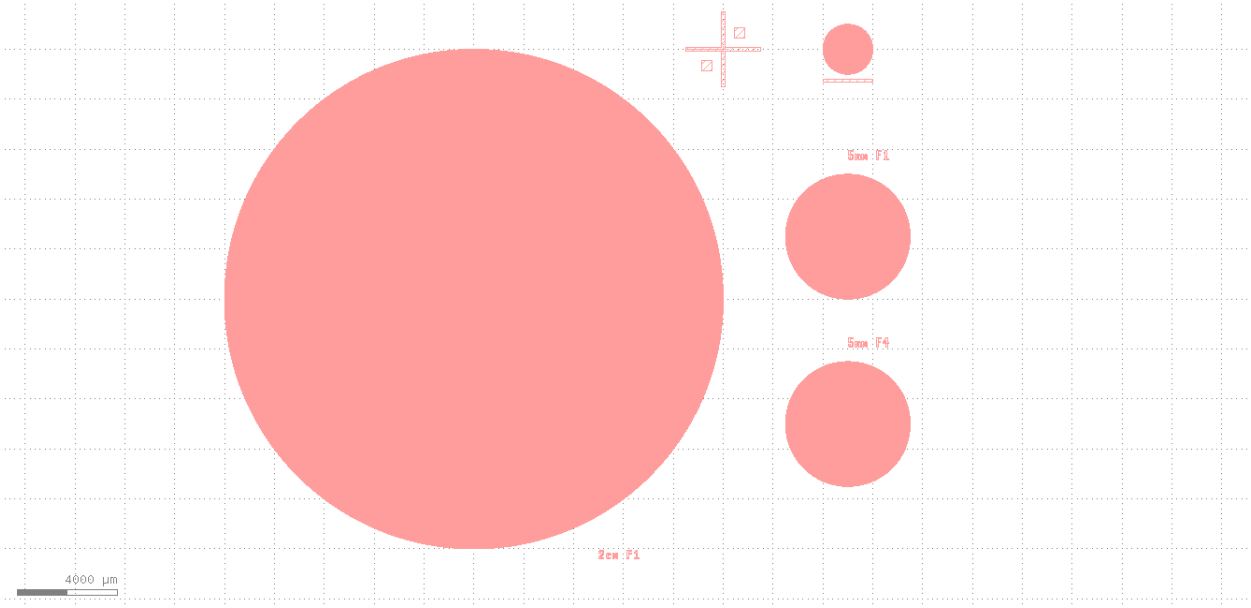

Figure 15: Raw GDS file of the layout of the 2cm design

The fabrication starts from the 2D GDS pattern which is selected from the user drive. The file is then converted using the Heidelberg software into a job file. Running the job file on the Heidelberg DWL66+ writes the processed GDS file directly with a laser into a layer of AZ1505 positive photoresist absorptive to ultraviolet laser light. The wafer is then developed in AZ726 photoresist developer for 1 minute. In this step the pattern written with the laser is revealed and the photoresist becomes a photomask for the etching step. The exposed areas of Silicon are then etched in Deep Reactive Ion Etch (DRIE) system to a desired depth in this case for 3um.

Following the etch step, the wafer is inspected in a Scanning Electron Microscope (SEM) to verify the quality of the fabrication process in which any meta-atom pillars that collapsed from DRIE can be seen. It is worth noting here that not that many pillars collapsed in the fabrication of 1cm and 2cm lenses. The resulting lab test found the devices to be virtually unimpaired due to the pillars collapse and the fabrication was found to be good. Finally, the SEM inspected wafer is taken to the optics lab and to record the devices' quantitative and qualitative performance. The quantitative performance is measured by Point Spread Function (PSF), using a point source which is an infra-red laser, the device is then benchmarked on how well it can focus laser light into a point. Intensity of light at a point is then measured to give a quantifiable result. The qualitative performance is measured using a Forward Looking Infra-Red (FLIR) camera, using a hotplate and USAF target as a source of light. The image recorded by FLIR camera is then judged by the operator on how sharp the image is, compared to standard diffractive optic.

9. MWIR doublet fabrication

In the case of MWIR doublet, there are two separate MWIR lenses to be fabricated. One lens is designed to operate under a higher field of view (a higher range of angles of the incident light). The other lens is designed to be used with a broader range of wavelengths, thus giving it what is referred to as a broadband capability. The fabrication of the MWIR doublet required two different GDS, cartoons of which are shown in the figures below.

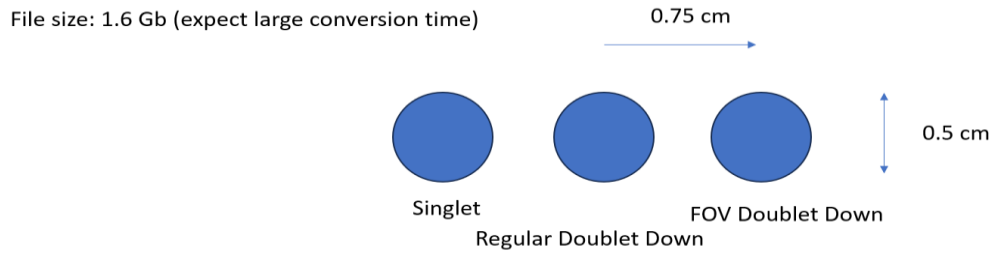

Figure 16: Wafer 1 GDS which includes the FOV doublet down

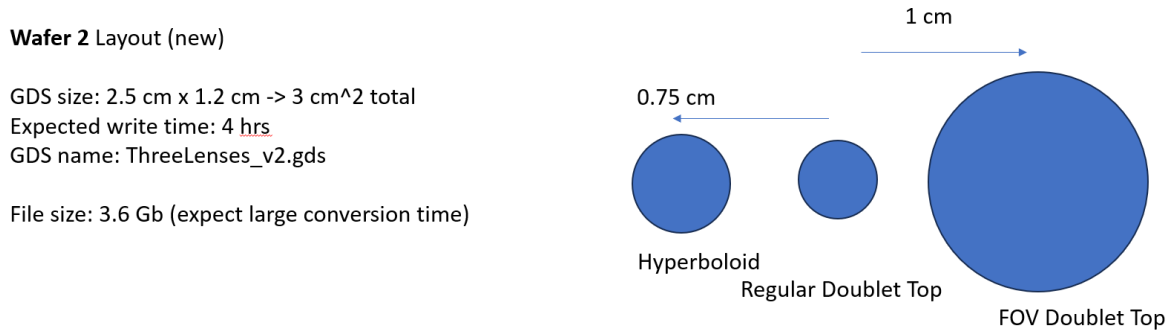

Figure 17: Wafer 2 GDS which includes the FOV doublet top

The fabrication starts from the 2D GDS patterns. To fabricate the doublet the two wafer have been processed individually and in a sequential manner. First Wafer 1 has done through wafer prep, lithography, development, pre DRIE ash, DRIE etch, resist strip, and SEM inspection. Wafer 1 was then tested in the optical lab as a single lens. If one lens is placed in the testing apparatus, the qualitative optical performance is expected to be worse than that if two lenses of the doublet were tested. This was later confirmed experimentally. Wafer 2 than got through the same steps as wafer one, and the fabrication process summary is given below. The converted GDS file of the desired wafer is written in a direct laser write system Heidelberg DWL 66+ where the exposed a layer of AZ1505 positive photoresist. The wafer is then developed in AZ726 photoresist developer for 1 minute. In this step the pattern written with the laser is revealed and the photoresist becomes a photomask for the etching step. The exposed areas of Silicon are then etched in Deep Reactive Ion Etch (DRIE) system to a desired depth of either 5um in case of MWIR doublet and for both wafers. Following the etch step, the wafer is inspected in a Scanning Electron Microscope (SEM) to verify the quality of the fabrication process in which any meta-atom pillars that still collapsed from DRIE can be seen. Finally, the SEM inspected wafer is taken to the optics lab and to record the devices' quantitative and qualitative performance. The quantitative performance is measured by Point Spread Function (PSF), using a point source

which is an infra-red laser, the device is then benchmarked on how well it can focus laser light into a point. Intensity of light at a point is then measured to give a quantifiable result. The qualitative performance is measured using a Forward Looking Infra-Red (FLIR) camera, using a hotplate and USAF target as a source of light. The image recorded by FLIR camera is then judged by the operator on how sharp the image is, compared to standard diffractive optic.

10. Golay Lens or Sparce Aperture fabrication

This design was chosen to test the theory of creating an effective larger aperture out of strategically placed smaller apertures. Although the apertures do not cover the whole wafer as seen on the Figure 18, if the source of Infra Red light is sufficiently far away and the focal length is sufficiently large, 35.8 cm in this case, the light will be lensed by all the apertures and will form one big lens, albeit at a cost of slightly lower resolution as compared to the lens covering the entire wafer. The real military application would require to scale up this design even further and fabricate portions of the Golay lens on seven individual wafers. The wafers can then be arranged on a jig that is itself transparent to IR light. These wafers spread out in a triangle pattern and the jig will then form effectively one big lens that is in theory capable of discerning a golf ball sized object at a distance of a football field length. The reason why the individual apertures are positioned in a triangle pattern is that this arrangement in theory gives the best image quality for the ratio of the surface area occupied by individual spread out aperture versus the total area of the wafer.

The fabrication of this Golay lens was somewhat different that any other lens that were fabricated for this work, as it actually required two layers. The first layer involved a negative photoresist that just patterned seven circles as an outline for where the apertures will later be. A layer of Chromium that is then deposited on the wafer binds to the silicon and goes on top of the

circles of resist, which is then dissolved in the liftoff step, forming perfectly circular openings where later the nanopillars are patterned during the second layer of the fabrication. Chromium is absorbent to the IR light and thus the fabricated device has 'isolated' lenses in a triangle arrangement.

Thus the fabrication starts with NR9G-3000 negative photoresist application. It is important to use negative photoresist in this step, because the developed photoresist must have a negative sidewall profile, in order for an easier liftoff process. A 20mm head, which is the fastest possible Heidelberg write head was then used to write just the circles on the wafer (no nanopillars) and it only took about 20 minutes. The photoresist is then post exposure baked for 1 minute on a hot plate, which is a critical step as was discovered. If the post exposure bake is not performed, then the all the resist will be developed away instead of forming a pattern. The photoresist then was developed for 40 seconds in AD 10 developer. A Chromium layer was then deposited using EVAP 2 metal evaporator in WNF to a target thickness of 200nm for the final device to be able to block out the IR light. The liftoff step, which just involves placing a wafer in a beaker of acetove for less than a minute was done to form the circular openings in the metal for the nanopillar meta lenses to be fitted precisely in the circles. From Figure 18 one can see striations on the Chromium metal that resembles grain boundaries. This is just an effect created in a metal layer during the deposition step. Since metal was deposited using a electron beam evaporation, in which chromium is evaporated from a solid crucible using a stream of electrons at 10kV which is then steered magnetically to form a melt pool in the crucible thus evaporating the metal. The hot Chromium in the gas phase then rises in the vacuum chamber of the tool and is then deposited on the cooler silicon wafer. Following liftoff the wafer is exposed to Hexamethyldisilazane (HMDS), a chemical that promotes the adhesion of photoresist to the wafer surface, after which

AZ 1512 is then spin coated on the wafer. A sparce aperture GDS is then converted in the Heidelberg tool to a kob file. The In the GDS design for this write, a small gap of 100um was left on the periphery of the circles necessary to form the undeveloped layer of photoresist in between the Chromium and patterned nanopillars. The undeveloped AZ 1512 thus forms a polymer barrier that ensures that all Chromium is covered in photoresist, which is necessary under the guidelines for DRIE tool use in Washington Nanofabrication Facility (WNF). No metal must be in the contact with the plasma in the tool in order to prevent metal contamination of the process chamber. The exposed areas of Silicon are then etched in Deep Reactive Ion Etch (DRIE) system to a desired depth in this case for 7.9um. Finally, the photoresist is stripped from the silicon nanopillars and the device is ready to test in an optical lab.

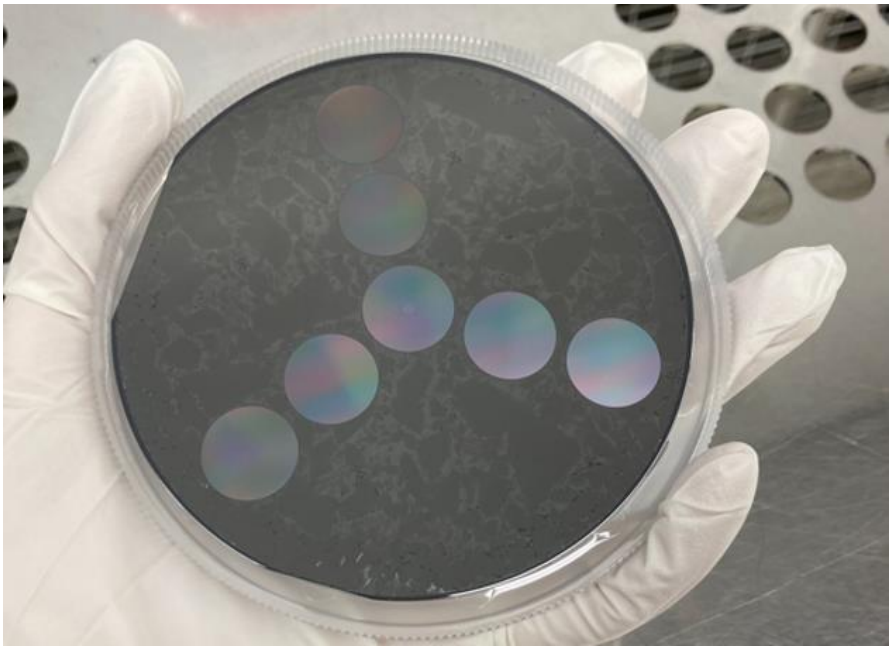

Figure 18: A cell phone camera image of the finished Golay lens

11. Very Large 8cm MWIR Aperture Fabrication

To truly test the limits of how big the aperture can be fabricated on a silicon wafer that is 4 inches (100mm) in diameter it is finally time to make a very large aperture that spans 8 centimeters in diameter. As mentioned earlier, it takes about 61 hours to cover to write the whole wafer using a high res head on Heidelberg DWL 66+. Therefore, attempting this design using the smallest head would be impractical, as the software will inevitably crash during the run. Thus, the choice was made to also write this meta lens with a 4mm head, which still takes about 360 minutes or 6 hours to complete, which is doable during an overnight slot and works well with tool reservation policy in Washington Nanofabrication Facility (WNF). This fabrication is different and simpler in a sense than a Golay Lens fabrication, since there is no need to write into the negative photoresist layer that will eventually become circular openings left for the writing nanopillars to pattern the apertures. The process starts with applying AZ 1512 photoresist directly to a blank silicon wafer. Then a 2D GDS pattern which is selected from the user drive is converted using the Heidelberg software into a job file. Running the job file on the Heidelberg DWL66+ writes the processed GDS file directly with a laser into a layer of AZ1512 positive photoresist absorptive to ultraviolet laser light. The wafer is then developed in AZ726 photoresist developer for 1 minute and 30 seconds. In this step the pattern written with the laser is revealed and the photoresist becomes a photomask for the etching step. The exposed areas of Silicon are then etched in Deep Reactive Ion Etch (DRIE) system to a desired depth in this case for 7.9um. It was found from the simulations that if the nanopillars are more spread out, i.e. have a larger periodicity, which was necessary for the desing to be compatible with writing using the 4mm head, the nanopillar height was needed to be increased to a target 7.9umm in order to cover 0 to

2π phase shift. In this case the height is chosen to be 7.9um and it dictates the etch depth into the silicon substrate during the Deep Reactive Ion Etching (DRIE) step of the meta lens fabrication.

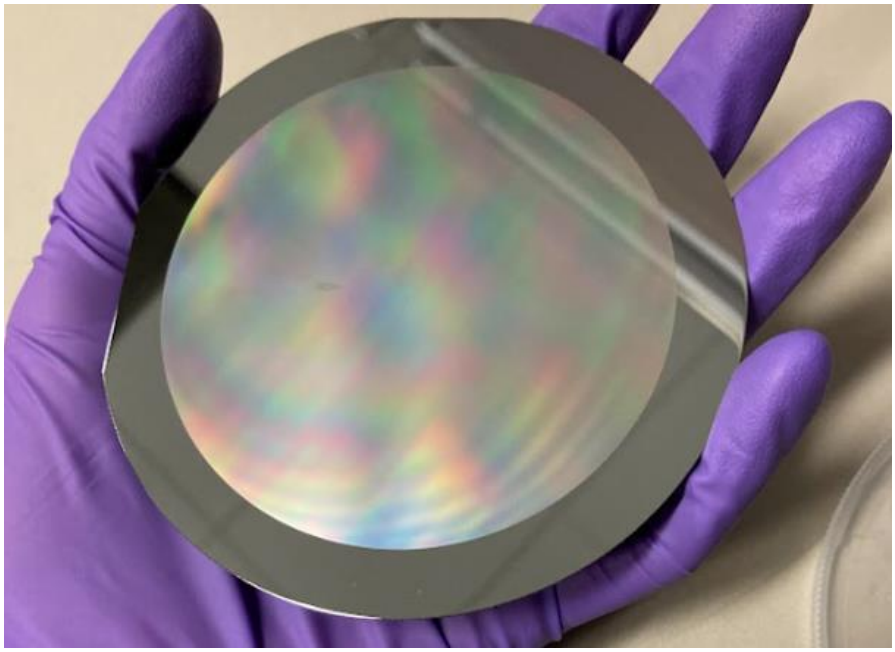

Figure 19: A cell phone camera image of the fabricated 8cm meta lens

The finished device must be handled extra carefully, since any scratch or scuff left on any of the surface of the ass-Si scatterer that forms the meta lens will degrade its performance when this device will be tested in the optical lab. That said, the device is somewhat forgiving towards the fabrication imperfections and if one to study the image carefully there is a small streak on the wafer, just left of center. It resulted from a photoresist unevenly covering the wafer during the application of AZ 1512 photoresist, that eventually got transferred to the wafer during DRIE etch step. Despite this imperfection, the device tested well, as will be shown in the Optical Results section of this work. To accommodate the large aperture and to reduce the effect of aliasing the F number was chosen to be 2 and thus the focal length for this wafer is 16 cm.

12. Optical lab measurement setup

Testing of the fabricated devices was done in a specialized optical lab that was set up in a different building from where the devices were fabricated. This optical lab has the capability of quantitatively measuring Point Spread Function (PSF) of the device as well as qualitatively measuring the device performance in terms of broadband (multi-wavelength) measurement as well as wide angle characterization. The PSF measurement set up is demonstrated in the image below [Figure 20].

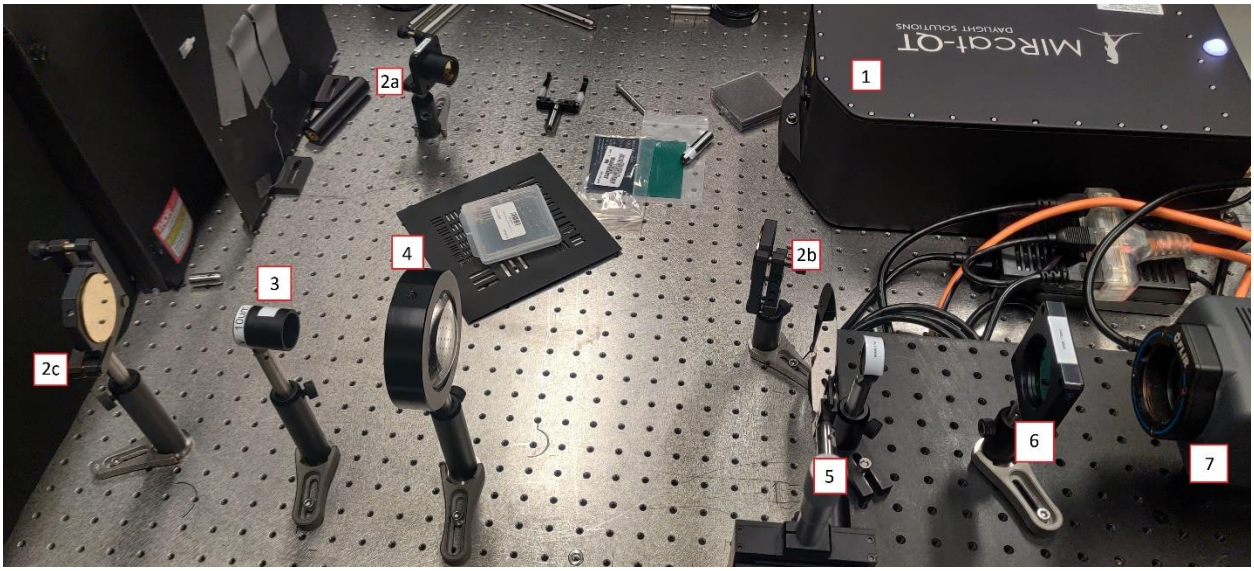

The image demonstrates a metal table with threaded holes separated by 1 inch from each other which provides the reader with a sense of scale for the setup. An Infra-Red laser [insert laser wavelength here] shown as 1 on the picture is producing a point source of light. It is important to mention that the laser beam spot size gets bigger slightly as it makes its way down the setup due to the natural divergence of the laser beam. Strategically placed mirrors 2a, 2b, and 2c then steer the laser beam so that it is perpendicular to the meta optic (shown as 5 on the image). However, in order to make a valid measurement of the PSF, the laser spot must cover the meta optic. For this reason, in this optical setup the laser beam spot is artificially made larger using

the optical lenses 3 and 4 on the picture. The light is then diffracted and manipulated by the meta atoms of the meta optic (5) and is passed on to the relay lens (shown as 6) which is required for this particular setup as the distance of the sensor of the Infra-Red camera (shown as 7) does not allow for the image to come into focus otherwise.

If done correctly, the laser beam that is broadened to cover the entire meta optic is then focused on a single point on the Infra-Red camera sensor. The procedure of focusing the light from the laser on a very tight spot on the sensor must be done in steps. First the camera takes a focused image of the surface of the silicon wafer with the meta optic to make sure that the meta optic is perfectly in line with the path of the laser beam. Then the focal distance is changed so that the laser beam is illuminating a spot in the center of the meta optic. As the beam spot gets smaller and smaller, the camera exposure (measured in milliseconds) needs to be lowered in order not to cause damage to the sensor. Finally, iterating these two steps, namely tightening the laser spot and lowering exposure, the laser beam is brought to its final spot size of about 20um or 4 pixels wide as captured by the Infra-Red camera sensor. The intensity of light at the pixel is measured and the result of the Point Spread Function is then recorded.

There is an alternative setup for performing the qualitative measurement of the quality of fabrication of the device, as well as measurement of broadband and wide angle performance of the meta optic. The same table is used as in the image above [Figure 20], however the setup is different. The hot plate is prepared in advance by heating it to 120 degrees C. Hot plate provides a known wavelength of Infra-Red light due to its black body radiation. A metal target with cutouts representing the US Air Force (USAF) pattern is placed downstream from the hot plate. As a result only the Infra-Red light, naturally produced by the heated hot plate that makes past the cold metal target can is passed on downstream towards the camera.

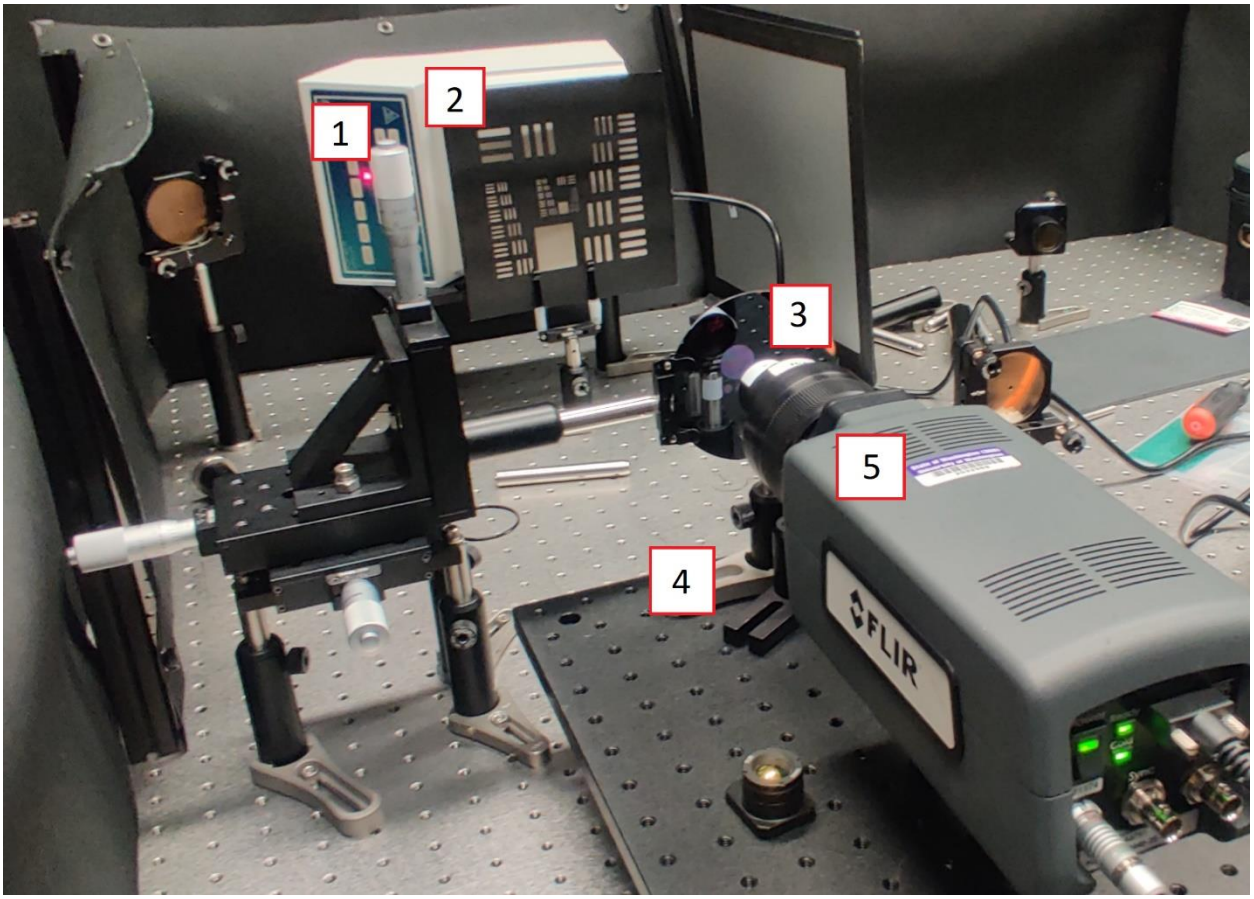

A meta optic is placed in front of the camera (shown as 3). First the camera takes a focused image of the surface of the silicon wafer with the meta optic to make sure that the center of the meta optic lens is perfectly in line with the camera. The focal distance is then changed in the increments of 0.05 inches of 0.1 inches in order to determine the optimal clarity of the image, provided the metal USAF target. This is achieved by moving the distance of the Infra-Red camera (shown as 5) from the meta optic. The camera is positioned on an adjustable stand and its distance can be changed by turning a knob with markers allowing for setting a precise distance. A relay lens (shown as 4) is again necessary for this particular setup as the distance of the sensor of the Infra-Red camera (shown as 7) does not allow for the image to come into focus otherwise. From taking repeated images at each focal distance the best image is selected as well as an image of the focal distance where image appears the sharpest. To determine the focal

distance the reading from the adjustable knob below the camera is taken and the reading at which the camera is focused on the surface of the wafer is subtracted. This distance is then compared to the designed focal distance of the meta optic.

13. Optical Results: A Qualitative and Quantitative Study

Quantitative PSF Measurements

In order to test how well the light is being focused to a point on various meta lenses, one must first test the pixel resolution of the sensor. The advertised resolution of the FLIR A6751 MWIR Cooled InSb camera used in the laboratory setup is 640x512 pixels and the pixel size is 15 micron/pixel. Using the image of a 5mm lens as a standard for length scale and calibrating the measuring length to register that the diameter of the lens should be exactly 5mm one can then measure the entire width of the frame from an image taken with no additional digital magnification. Converting 9.55mm to microns gives 9550 um and the number of pixel on the horizontal should be 640. Then dividing these two numbers results in 14.9 um/px. This is very close to advertised pixel size of the sensor and thus this number will be a valid pixel size to use for PSF measurement.

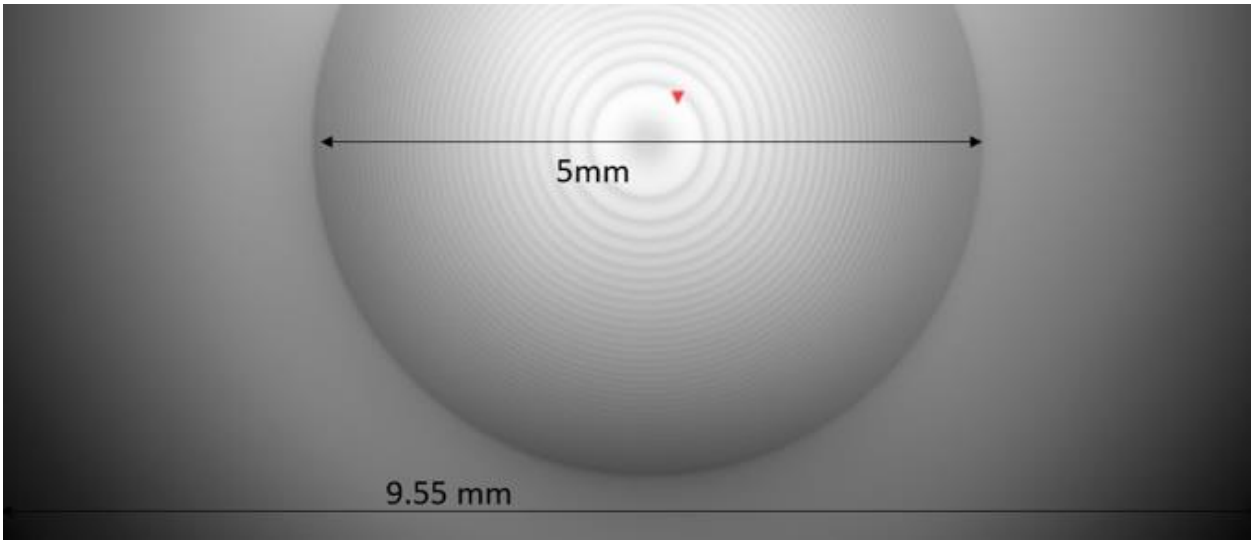

Figure 22 Pixel size measurement of the camera sensor

Four different lenses were used to measure PSF. Please refer to the lab measurement setup for reference to how this data was taken. The laser, a Daylight Solutions MIRcat MWIR QCL laser is guided by a set of strategically positioned mirrors until it hits the meta lens. Then the meta lens is focusing the laser beam to a very tight spot directly on the camera sensor, ideally letting the laser beam converge to a point.

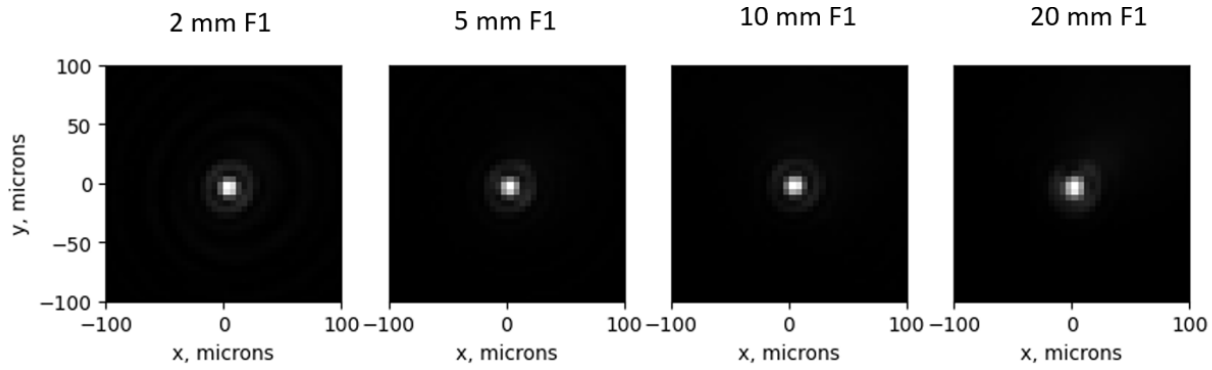

Figure 23 PSF measurements for four different meta lenses fabricated for this work

As one can note the PSF graphs for all four lenses did not converge to the exact point. The comparison is made on Figure 24.

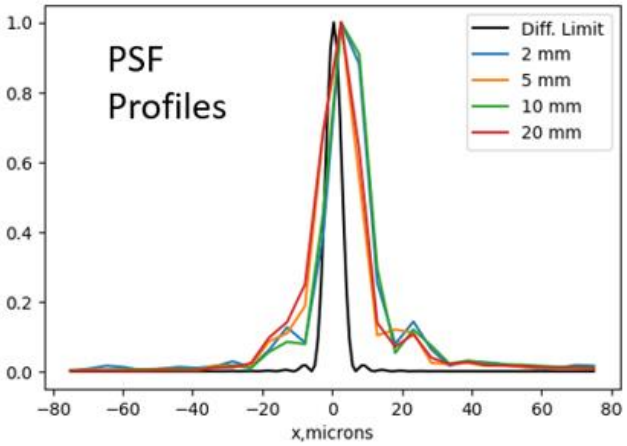

Figure 24 PSF profile peaks as compared to the diffraction limit. Vertical axis is intensity

There are at least two explanations why the PSF graphs are not in the ideal width of a diffraction limit for the meta lenses. First, the lenses were made in a microfabrication facility and required many individual steps. During each step there bound to be imperfections or fabrication errors that get added up to a final and imperfect device. The second explanation is that the meta optic when placed in the PSF setup may not actually be mounted strictly perpendicular to the incoming laser beam. Any misalignment in the laboratory set up negatively affects the PSF graph and broadens the intensity peak.

14. Qualitative FLIR Images

Before discussing the actual images taken with the aid of fabricated meta lenses and the laboratory optical setup it is important to mention that the source of Infra Red light is not ideal for almost all lenses. For all the measurements where there are images of vertical and horizontal lines a hot plate was used for the source of IR light, as shown in the measurement setup section. It has been mentioned previously that the hotplate, or for that matter any source of blackbody radiation radiates light that has a peak wavelength but the emission is also a wide distribution of wavelengths (Figure 2). Therefore, any measurement done with a hotplate is considered to be broadband imaging. All the fabricated lenses, except the fabricated MWIR doublet meta lens, were designed to be used with a single wavelength of light of 4.5 micron. Even though the hotplate tests are not the ideal testing scenario, the resulting images came out sufficiently well and the target features, such as USAF target stripes and Husky on the UW Husky target were all discernable.

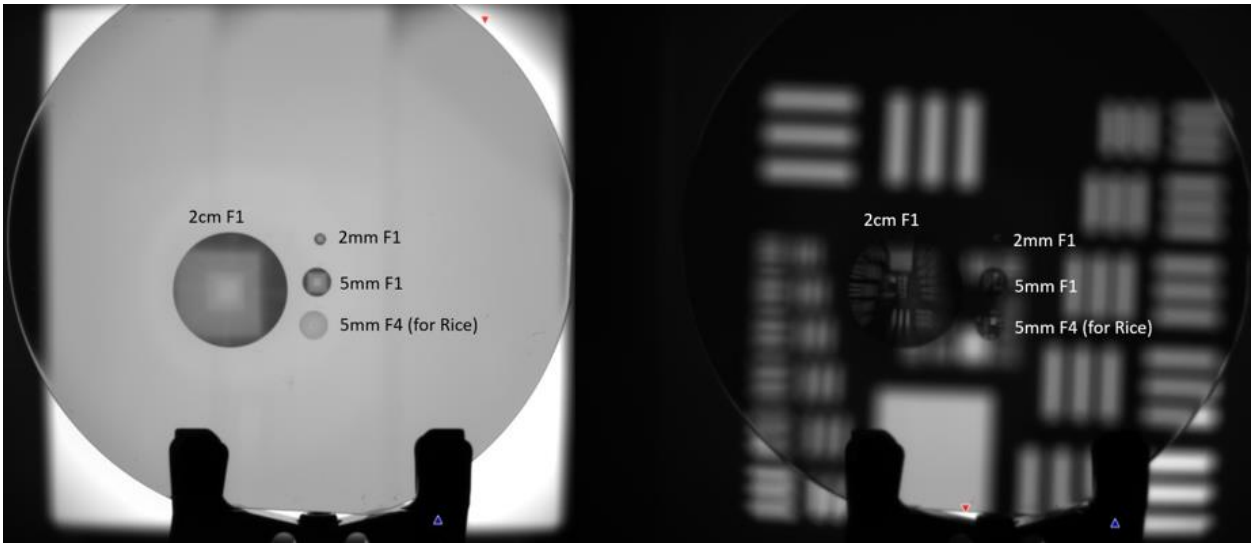

Figure 25. Comparison between the lenses. Camera is focused on the meta lenses to assess which lens have higher transmission (left) and focused on the background (right)

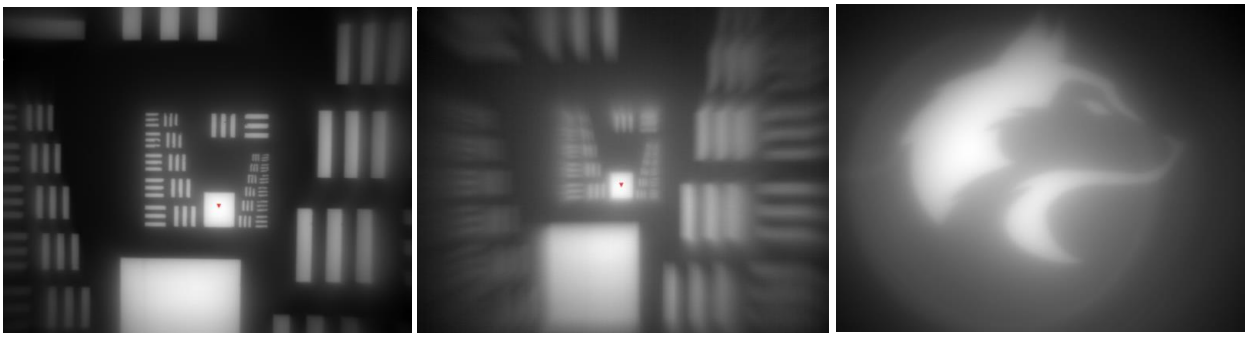

Figure 26. A comparison between refractive compound lens of d=25mm f=25mm(left) and d=8cm f=16cm meta lens (center) using USAF metal target and d=8cm f-16cm Husky target

References:

[1] “Metalenses: Meta Optics: Meta Optical Elements: Nilt.” NIL Technology, 25 Sept. 2023.

[2] Systems, ARC Centre of Excellence for Transformative Meta-Optical. “Meta-Optics: The Disruptive Technology You Didn’t See Coming.” Phys.org

[3] Opti, Melanie. MATERIALS for INFRARED OPTICS. 1 Oct. 2016.

[4] Heaton, Wyatt. “Night Vision vs. Thermal Optics: What You Need to Know.” www.agmglobalvision.com, 14 Mar. 2020.

[5] “Security and Surveillance – Thermal Camera Embedded on Drone.” AltiGator Drone & UAV Technologies, 16 Jan. 2015.

[6] Rangwala, Sabbir. “Thermal Cameras Gain Acceptance for ADAS and Autonomous Cars.” Forbes, 28 Oct. 2022.

[7] Shih, Ko-Han, and Kyle C. Renshaw. “Optica Publishing Group.” Opg.optica.org, 31 Dec. 2021.

[8] A. Ayari-Kanoun et al. “Silicon nanostructures with very large negatively tapered profile” Journal of Vacuum Science & Technology B